TU Delft
Delft University of Technology

Department of Civil Engineering
Hydraulic and Geotechnical Engineering Division
Hydromechanics Section

Consolidation theory and rheology of mud

A literature survey

L.M. Merckelbach

report no. 9-96

Ph.D. student, Hydromechanics Section, Department of Civil Engineering, Delft University of Technology, P.O. Box 5048, 2600 GA, the Netherlands. Tel. +31 15 278 40 70; Fax +31 15 278 59 75; E-mail: L.Merckelbach@ct.tudelft.nl

Abstract

In the framework of project *Strength evolution of soft consolidating mud layers*, financially supported by the Netherlands Foundation of Technology, a literature survey on consolidation theory and rheological modelling of mud was carried out.

A consolidation theory, focussed on the Gibson equation (Gibson *et al.*, 1967), is presented. The solution of Gibson's one-dimensional finite strain consolidation equation requires closure relations for the effective stress and the permeability. It is assumed that both relations are functions of the void ratio only.

However, the consolidation of soft soils cannot be modelled adequately with these assumptions, since effects as aging, channeling, creep, formation and break-up of flocs, for example, are not taken into account. The incorporation of a rheological model into the consolidation model can result in a better modelling of consolidating mud layers.

From this point of view, various rheological models are presented, starting with simple models that become increasingly complex. The complex models incorporate thixotropy and yield stress to describe rheolocial complex fluids as mud.

Experimental evidence of a relationship between effective stress and yield stress is presented. Topics for future research are indicated.

Contents

Chapter 1

Introduction

In the framework of the project *Strength evolution of soft consolidating mud layers* a literature survey on sedimentation and consolidation as well as the rheological modelling of mud is carried out.

The aim of this report is to gain insight into (the theoretical aspects of) the consolidation of mud and its rheological modelling.

Outline

In the second chapter attention is paid to the derivation of a one-dimensional finite strain, self-weight consolidation equation in Eulerian coordinates. This equation is equivalent to Gibson's consolidation equation (Gibson *et al.*, 1967) written in material coordinates. Material coordinates are more convenient with respect to solving the equation numerically. It is shown that both Kynch's sedimentation equation (Kynch, 1952) and Terzaghi's consolidation equation (Terzaghi, 1943) are special cases of this one-dimensional consolidation equation.

Pane and Schiffman (1985) modified Gibson's consolidation equation by generalizing the effective stress principle in order to link sedimentation and consolidation.

From the linearized Gibson equation a relation between effective stress and void ratio is obtained. With this relation the boundary conditions are specified, which are necessary to solve the Gibson equation.

In Chapter 3 some principles of rheology are presented. Introducing various (empirical) models, various types of rheological behaviour are illustrated. Special attention is paid to thixotropic behaviour.

In Chapter 4 experimental evidence of a relation between yield stress and effective stress is presented, linking consolidation and rheology. Some topics for future research are given and the conclusions of this literature survey are drawn.

Chapter 2

Theory of sedimentation and consolidation

2.1 Introduction

The process of soil formation consists of three stages. The first stage is the sedimentation of a suspension. A suspension may be considered as a mixture of soil particles in water where the dilution is such that the particles are fully supported by fluid, although the movement of a certain particle may be influenced by the proximity of other particles. With increasing concentration the particles begin to support each other partially, which marks the transition to the second stage: consolidation. In this phase the soil is formed and the effective stress increases while the pore-water pressure and the void ratio decrease. This process proceeds until the effective stress does not change anymore. However, during the third stage, the void ratio may continue to decrease. This process is called creep or secondary consolidation.

This chapter is devoted to the modelling of the first two stages: sedimentation and consolidation. First a general consolidation equation in a Eulerian coordinate system is discussed. Transformation of this equation into a Lagrangian-like coordinate system, which is much more convenient when solving the equation, yields the Gibson equation (Gibson *et al.*, 1967). Subsequently, it is shown that Terzaghi's classical theory of consolidation (Terzaghi, 1943) and Kynch's theory of sedimentation (Kynch, 1952) are special cases of the Gibson equation. The generalization of the effective stress principle in order to link sedimentation and consolidation by Pane and Schiffman (1985) is discussed. From the linearized Gibson equation a relation between the effective stress and the void ratio is obtained. This relation is used to specify the boundary conditions.

2.2 One-dimensional consolidation theory

A one-dimensional consolidation equation is derived in the Eulerian coordinate system (x,τ). The x-axis is taken positive in the upward direction. In the Eulerian coordinate system τ denotes time.

It is assumed that the soil is completely saturated and the mixture consists of a solid phase

and a liquid phase only. Moreover the mixture is considered to be incompressible. Therefore the summation of the liquid fraction ϕ_f and the solid fraction ϕ_s equals unity. The fractions are related to the void ratio e according to

$$\phi_s = \frac{1}{1+e} \quad \text{and} \quad \phi_f = \frac{e}{1+e}. \tag{2.1}$$

The vertical equilibrium of the two phase mixture can be written as

$$\frac{\partial \sigma}{\partial x} = -\frac{e}{1+e}\rho_f g - \frac{1}{1+e}\rho_s g, \tag{2.2}$$

where σ is the total stress, g is the acceleration due to gravity and ρ_f and ρ_s represent the densities of the fluid and solids.

Conservation of mass reduces to conservation of volume occupied by particles, if it is assumed that, in addition to incompressibility, the densities are constant in time and space. Conservation of sediment volume yields the continuity equation

$$\frac{\partial \phi_s}{\partial \tau} + \frac{\partial}{\partial x}(v_s \phi_s) = 0, \tag{2.3}$$

which can be written as

$$\frac{\partial e}{\partial \tau} = (1+e)^2 \frac{\partial}{\partial x}\left(v_s \frac{1}{1+e}\right), \tag{2.4}$$

where v_s is the velocity of the particles relative to the datum plane and it is taken the positive in positive x direction, see Figure 2.1. Although a continuity equation can be formulated for the pore fluid as well, no additional information is gained since the assumptions made above result in dependent formulations.

The motion of the pore fluid relative to the particles is usually modelled by Darcy's law, which is written as

$$\frac{e}{1+e}(v_f - v_s) = -k \frac{1}{\rho_f g} \frac{\partial p_e}{\partial x}, \tag{2.5}$$

where v_f is the velocity of the fluid, k is the permeability of the soil and p_e is the excess pore pressure defined by the difference of the pore-water pressure and the steady-state (hydrostatic) pore-water pressure:

$$p_e = p - p_{ss}. \tag{2.6}$$

The velocity $(v_f - v_s)$ is usually called as the effective velocity, which is equal to the difference in velocity between the particles and the fluid, see also Figure 2.1.

For reasons of continuity the volume flux of the mixture equals zero, so that,

$$\phi_s v_s + \phi_f v_f = 0, \tag{2.7}$$

or,

$$\frac{1}{1+e} v_s + \frac{e}{1+e} v_f = 0. \tag{2.8}$$

Equation (2.8) can be rewritten to yield the relationship

$$\frac{e}{1+e}(v_f - v_s) = -v_s. \tag{2.9}$$

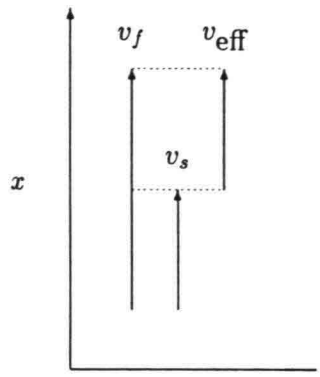

Figure 2.1: Definition sketch of particle and fluid velocities

Substituting from (2.9) and using (2.6), equation (2.5) yields

$$v_s = \frac{k}{\rho_f g}\frac{\partial p}{\partial x} + k. \tag{2.10}$$

Subsequently, using the effective stress principle

$$\sigma = \sigma' + p, \tag{2.11}$$

equation (2.10) can be written as

$$v_s = \frac{k}{\rho_f g}\left(\frac{\partial \sigma}{\partial x} - \frac{\partial \sigma'}{\partial x}\right) + k. \tag{2.12}$$

Here, σ represents the total stress, σ' represents the effective stress, i.e. an interparticle stress. The effective stress is defined such that the deformations of the soil are determined the effective stress determines (Terzaghi, 1943).

Combining equations (2.2), (2.4) and (2.12) results in a one-dimensional consolidation equation in Eulerian coordinates for the void ratio e:

$$\frac{\partial e}{\partial \tau} + (1+e)^2\left(\frac{\rho_s}{\rho_f} - 1\right)\frac{\partial}{\partial x}\left[\frac{k}{(1+e)^2}\right] + \frac{(1+e)^2}{\rho_f g}\frac{\partial}{\partial x}\left[\frac{k}{(1+e)}\frac{\partial \sigma'}{\partial x}\right] = 0. \tag{2.13}$$

The numerical solution of this non-linear partial differential equation is complex as a result of moving boundaries. If, for example, a consolidation experiment in a column is simulated, the uppermost interface of the mixture drops when time increases and so does the corresponding boundary in a numerical model. This problem can be avoided by introducing Lagrangian coordinates. A coordinate system that is closely related to the Lagrangian system is the *material* coordinate system, which appears to be more suitable to solve (2.13).

Material coordinate system

Consider a consolidation column with an initial height equal to x_0, see Figure 2.2 (a), left column. The right column in this figure represents the same column in material coordinates. The material coordinate z indicates the volume of solids per unit area above the datum point. It is therefore defined by

$$z(x) = \int_0^x \frac{\mathrm{d}x'}{1+e(x',\tau)}. \tag{2.14}$$

The time t in the material coordinate system is equal to τ, so that

$$t(\tau) = \tau. \tag{2.15}$$

After some time, at $t = t_1$, the consolidation has proceeded, see Figure 2.2 (b), left column. As a result of the consolidation process the top of the column has dropped to level x_1 and the original slice has become thinner as water has escaped. Since no solid material is added or removed, the height of column in z space does not change and therefore the boundaries do not move. However, the slice thickness does change as can be seen in the sketch. The ratio $\partial z/\partial x$ follows by rewriting (2.14):

$$\frac{\partial z}{\partial x} = \frac{1}{1+e(x,\tau)}. \tag{2.16}$$

For the transformation from the Eulerian coordinate system in the material coordinate system the following transformation rules have to be obeyed:

$$\frac{\partial}{\partial x} = \frac{\partial}{\partial z}\frac{\partial z}{\partial x} + \frac{\partial}{\partial t}\frac{\partial t}{\partial x} \tag{2.17}$$

and

$$\frac{\partial}{\partial \tau} = \frac{\partial}{\partial z}\frac{\partial z}{\partial \tau} + \frac{\partial}{\partial t}\frac{\partial t}{\partial \tau}. \tag{2.18}$$

Substituting from (2.16) equation (2.17) becomes

$$\frac{\partial}{\partial x} = \frac{1}{1+e}\frac{\partial}{\partial z}, \tag{2.19}$$

since $\partial t/\partial x = 0$. Subsequently, substituting from (2.14) and interchanging differentiation and integration, into (2.18) becomes

$$\frac{\partial}{\partial \tau} = \frac{\partial}{\partial t} + \int_0^x \frac{\partial}{\partial \tau}\left[\frac{1}{1+e}\right]\mathrm{d}x'\frac{\partial}{\partial z}. \tag{2.20}$$

Equation (2.20) can be simplified by substituting from the continuity equation (2.4), which results in

$$\frac{\partial}{\partial \tau} = \frac{\partial}{\partial t} - \frac{v_s}{1+e}\frac{\partial}{\partial z}. \tag{2.21}$$

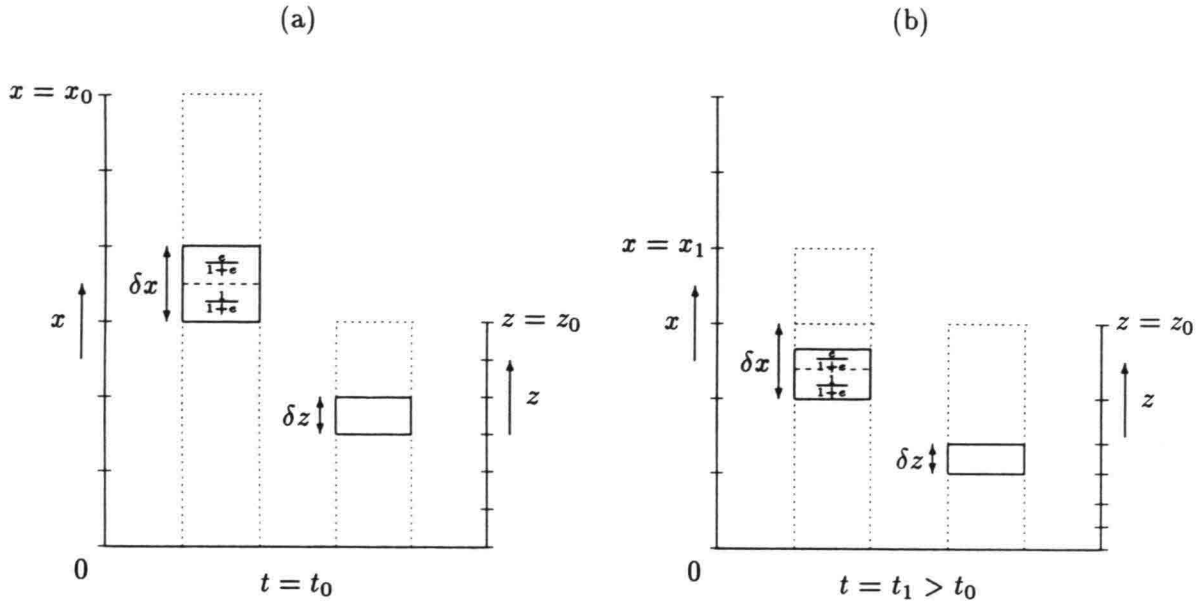

Figure 2.2: Definition sketch of a Lagrangian coordinate system

Gibson's consolidation equation

The most straightforward method to obtain the consolidation equation in material coordinates is by applying the transformation rules (2.19) and (2.21) to the Eulerian equation (2.13). Elaborating the result in order to obtain a compact equation is quite cumbersome. Transformation of the continuity equation (2.4) in material coordinates, followed by substitution of the (transformed) equations (2.2) and (2.12), simplifies the mathematical operations significantly. The latter approach is taken in the following.

Applying the transformation rules (2.19) and (2.21) to (2.4) yields

$$\frac{\partial e}{\partial t} - \frac{\partial v_s}{\partial z} = 0. \tag{2.22}$$

Subsequently, substituting the vertical equilibrium equation (2.2) into the Darcy model (2.12) yields, after applying the transformation rules

$$v_s = \left(1 - \frac{\rho_s}{\rho_f}\right) \frac{k}{1+e} - \frac{k}{\rho_f g(1+e)} \frac{\partial \sigma'}{\partial z}. \tag{2.23}$$

Combining the equations (2.22) and (2.23) yields

$$\frac{\partial e}{\partial t} + \left(\frac{\rho_s}{\rho_f} - 1\right) \frac{\partial}{\partial z}\left[\frac{k}{1+e}\right] + \frac{\partial}{\partial z}\left[\frac{k}{\rho_f g(1+e)} \frac{\partial \sigma'}{\partial z}\right] = 0. \tag{2.24}$$

Equation (2.24) still contains, additional to the variable e, two unknowns, namely the permeability k and the effective stress σ'. In classical soil mechanics it is assumed that both k and σ' are a function of the void ratio only and that empirical formulations can be used. With this assumption history effects, channeling and formation and break up of aggregates

are excluded from the model. Based on these assumptions equation (2.24) can be rewritten as

$$\frac{\partial e}{\partial t} + \left(\frac{\rho_s}{\rho_f} - 1\right) \frac{\mathrm{d}}{\mathrm{d}e}\left[\frac{k(e)}{1+e}\right] \frac{\partial e}{\partial z} + \frac{\partial}{\partial z}\left[\frac{k(e)}{\rho_f g(1+e)} \frac{\mathrm{d}}{\mathrm{d}e}\left[\sigma'(e)\right] \frac{\partial e}{\partial z}\right] = 0, \tag{2.25}$$

which is known as the Gibson equation (Gibson *et al.*, 1967).

Applying again the simplifications $k, \sigma' = f(e)$ to the consolidation equation (2.13) yields the equivalence of the Gibson equation in Eulerian coordinates:

$$\frac{\partial e}{\partial \tau} + (1+e)^2 \left(\frac{\rho_s}{\rho_f} - 1\right) \frac{\mathrm{d}}{\mathrm{d}e}\left[\frac{k(e)}{(1+e)^2}\right] \frac{\partial e}{\partial x} + \frac{(1+e)^2}{\rho_f g} \frac{\partial}{\partial x}\left[\frac{k(e)}{(1+e)} \frac{\mathrm{d}}{\mathrm{d}e}[\sigma'(e)] \frac{\partial e}{\partial x}\right] = 0. \tag{2.26}$$

A special case of the 1-D consolidation equation: Terzaghi's consolidation theory

Terzaghi (1943) derived a theory of consolidation, based on a linear stress-strain relation, a continuity equation, Darcy's law and the infinitesimal deformation principle. Moreover the theory neglects self-weight consolidation.

Terzaghi's consolidation equation is written in Eulerian coordinates as

$$\frac{\partial \sigma'}{\partial \tau} - \left[\frac{k(1+e)}{\rho_f g a_v}\right] \frac{\partial^2 \sigma'}{\partial x^2} = 0, \tag{2.27}$$

where a_v is a coefficient of compressibility, defined as

$$a_v = -\frac{\partial e}{\partial \sigma'}. \tag{2.28}$$

In order to show the relationship between Terzaghi's equation and the 1-D consolidation equation, the consolidation equation in Eulerian coordinates (2.26) will be rewritten and compared with equation (2.27).

Self-weight consolidation can be neglected by taking $\rho_s = \rho_f$, which eliminates the convective term of (2.26), so that Gibson's equation in Eulerian coordinates reduces to

$$\frac{\partial e}{\partial \tau} + \frac{(1+e)^2}{\rho_f g} \frac{\partial}{\partial x}\left[\frac{k(e)}{(1+e)} \frac{\mathrm{d}}{\mathrm{d}e}[\sigma'(e)] \frac{\partial e}{\partial x}\right] = 0, \tag{2.29}$$

In Terzaghi's theory it is assumed that the permeability k is constant during consolidation, which simplifies (2.29). However, this equation is non-linear, which can be seen when the equation is expanded. Neglecting this non-linear term yields

$$\frac{\partial e}{\partial \tau} + k \frac{(1+e)}{\rho_f g} \frac{\partial^2 \sigma'}{\partial x^2} = 0. \tag{2.30}$$

Substituting from (2.28), yields Terzaghi's equation (2.27).

A special case of the 1-D consolidation equation: Kynch's sedimentation theory

Kynch's theory of sedimentation (Kynch, 1952), describes the process of hindered settling during a one-dimensional sedimentation process. The main assumption is that at any point in the dispersion the settling velocity v_s only depends on the local concentration by mass c. The settling process is then determined entirely by a continuity equation, without knowing the details of the forces on the particles.

Kynch's sedimentation equation reads

$$\frac{\partial c}{\partial \tau} + W(c)\frac{\partial c}{\partial x} = 0 \tag{2.31}$$

where

$$W(c) = \frac{\mathrm{d}}{\mathrm{d}c}(v_s c). \tag{2.32}$$

In order to compare (2.31) with the 1-D consolidation equation (2.26), Kynch's equation is written in void ratio rather than in concentration. The relation between the concentration by mass and the void ratio is given by

$$c = \frac{\rho_s}{1+e}. \tag{2.33}$$

Transformation of (2.31) yields

$$\frac{\mathrm{d}c}{\mathrm{d}e}\frac{\partial e}{\partial \tau} - (1+e)^2\frac{\mathrm{d}}{\mathrm{d}e}\left[\frac{v_s}{1+e}\right]\frac{\mathrm{d}c}{\mathrm{d}e}\frac{\partial e}{\partial x} = 0, \tag{2.34}$$

which can be reduced to the continuity equation (2.4).

Where Darcy's law is used to model the particle–fluid interaction, Kynch assumes that the settling velocity is determined by the concentration (or void ratio) only. The relation between v_s and Darcy's k is given by (2.12), and reads in more elaborated form

$$v_s = k\left[\frac{1}{1+e}(1-\frac{\rho_s}{\rho_f}) - \frac{1}{\rho_f g}\frac{\partial \sigma'}{\partial x}\right]. \tag{2.35}$$

Since in Kynch's theory v_s is a function of e only, the derivative of the effective stress with respect to x is discarded and therefore (2.35) reduces to (Been, 1980)

$$v_s = \frac{k}{1+e}(1-\frac{\rho_s}{\rho_f}). \tag{2.36}$$

Substituting (2.36) into the continuity equation (2.4) yields

$$\frac{\partial e}{\partial \tau} + (1+e)^2\left(\frac{\rho_s}{\rho_f}-1\right)\frac{\mathrm{d}}{\mathrm{d}e}\left[\frac{k(e)}{(1+e)^2}\right]\frac{\partial e}{\partial x} = 0. \tag{2.37}$$

This equation is obtained from the 1-D consolidation equation (2.26) by leaving out the diffusive (third) term. The assumption that no effective stresses exist during sedimentation ($\sigma' = 0$) is a sufficient condition to obtain Kynch's model.

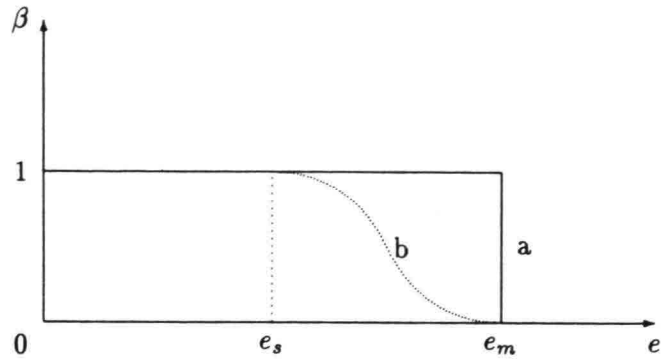

Figure 2.3: Forms of the constitutive relationship $\beta(e)$

2.2.1 Linking theory

Pane and Schiffman (1985) note that an 'intermediate region' of soil densities has been observed in laboratory sedimentation experiments with remote-sensed density measurements (Been, 1980). This intermediate region, which is characterized by rapid changes in concentration with depth, is associated with effective stresses which are not fully active yet. Therefore Pane and Schiffman generalized the effective stress principle by postulating

$$\sigma = \beta(e)\sigma' + p. \tag{2.38}$$

According to Pane and Schiffman the generalized principle of effective stress substituted into Gibson's consolidation equation (2.25), explains, from a mechanical point of view, the behaviour of soil–water mixtures. The resulting model makes possible the simultaneous modelling of sedimentation and consolidation.

The interaction coefficient β is a monotonic function of the void ratio. In Figure 2.3 a possible form of β is shown, however its real shape has never been investigated (Toorman, 1994).

The interaction coefficient is equal to zero for values of the void ratio greater than e_m. In this case the particles or particle aggregates are so distant that their interactions are negligible and the mixture behaves as a dispersion. For values of the void ratio less than e_s the interaction coefficient equals unity, indicating that the effective stress is fully developed and the mixture behaves as a soil. For values of the void ratio between e_m and e_s the mixture behaves neither as a dispersion nor as a soil, which is expressed by an interaction coefficient that gradually varies from unity to zero. The classical effective stress principle (2.11) is obtained by an abrupt change in β from unity to zero at $e = e_m$.

Assuming the validity of (2.38) the one dimensional consolidation equation (2.25)[1] is

[1]For reasons of consistency with the article of Pane and Schiffman, the consolidation equation in material coordinates is used rather than its equivalence in Eulerian coordinates.

extended to become

$$\frac{\partial e}{\partial t} + \left(\frac{\rho_s}{\rho_f} - 1\right) \frac{\mathrm{d}}{\mathrm{d}e}\left[\frac{k}{1+e}\right] \frac{\partial e}{\partial z} + \frac{\partial}{\partial z}\left[\frac{k}{\rho_f g(1+e)} \beta \frac{\mathrm{d}\sigma'}{\mathrm{d}e} \frac{\partial e}{\partial z}\right] + \frac{\partial}{\partial z}\left[\frac{k}{\rho_f g(1+e)} \sigma' \frac{\mathrm{d}\beta}{\mathrm{d}e} \frac{\partial e}{\partial z}\right] = 0. \tag{2.39}$$

For $e > e_m$ (2.39) reduces to an equivalence of Kynch's equation of sedimentation, as shown in the previous subsection. For $e < e_s$ the soil–water mixture is truly a soil: the effective stresses are fully active. In this case (2.39) reduces to the Gibson equation (2.25). For $e_m < e < e_s$ the soil–water mixture is in a transitional phase. In this phase the pore fluid velocity can be relatively high, so that the drag stresses are comparable with the effective stress. For this case the complete equation (2.39) has to be used.

Discussion

Pane and Schiffman generalized Terzaghi's effective stress principle, from a mechanical point of view. Verruijt (1984) generalized the effective stress principle by taking into account a small compressibility of the pore fluid and the particles.

He introduced a so-called intergranular stress, defined by

$$\bar{\sigma} = \sigma - p. \tag{2.40}$$

The change of volume is given by

$$\frac{\Delta V}{V} = -\frac{1}{K}\Delta\bar{\sigma} - \frac{1}{K_s}\Delta p, \tag{2.41}$$

where ΔV is the change of volume, V is a control volume, K and K_s are total compression modulus and the particle compression modulus, respectively.

Verruijt (1984) shows that the effective stress is generalized to

$$\sigma = \sigma' + (1 - \frac{K}{K_s})p. \tag{2.42}$$

This expression is also obtained by Biot and Willis (1957), Skempton (1960) and Tuncay and Corapciglu (1995).

If the total compression modulus is much smaller than the compression modulus of the particles, this is $K/K_s \to 0$, (2.42) reduces to Terzaghi's effective stress principle. This is the case when compression results in structural changes, due to sliding and rolling of the particles.

Especially in Pane and Schiffman's intermediate region, sliding and rolling of the particles is likely to occur, so that Terzaghi's effective stress principle is valid. Besides, the reduction factor multiplies the pore water pressure, rather than the effective stress. Thus the profit of the interaction coefficient of Pane and Schiffman can only be seen in the perspective of numerically solving the Gibson equation.

2.3 The relationship between effective stress and void ratio

Gibson's consolidation equation (2.25) is written as

$$\frac{\partial e}{\partial t} + \left(\frac{\rho_s}{\rho_f} - 1\right) \frac{\mathrm{d}}{\mathrm{d}e}\left[\frac{k(e)}{1+e}\right] \frac{\partial e}{\partial z} + \frac{\partial}{\partial z}\left[G(e)\frac{\partial e}{\partial z}\right] = 0, \tag{2.43}$$

where

$$G(e) = \frac{k(e)}{\rho_f g(1+e)} \frac{\mathrm{d}}{\mathrm{d}e}\left[\sigma'(e)\right] \tag{2.44}$$

It is likely that $G(e)$ is much less sensitive to changes in void ratio than its constituent terms. This suggests that taking G to be a constant may be a reasonable approximation for many clays (Gibson *et al.*, 1981).

A sensitivity analysis can be carried out to assess the validity of taking G to be a constant. Widely used empirical formulations for the relations $e - \sigma'$ and $k - e$ are, see e.g. (Hu, 1990)

$$e = A_p \left(\frac{\sigma'}{\sigma_r}\right)^{-B_p} \qquad \text{and } \sigma_r = 1 \text{ Pa} \tag{2.45}$$

$$\frac{k}{k_r} = A_k e_k^B \qquad \text{and } k_r = 1 \text{ m/s} \tag{2.46}$$

Considering mud from Lake Ketel (The Netherlands), the empirical relations give reasonable results for a small range of void ratios, i.e. $6 < e < 18$. The corresponding coefficients are tabulated in Table 2.1

Table 2.1: Empirical parameters for Lake Ketel mud, (Cornelisse *et al.*, 1993)

A_p	=	41.39
B_p	=	0.416
A_k	=	$7.09 \cdot 10^{-9}$
B_k	=	2.767

With these values $k(e)$, $\sigma'(e)$ and $G(e)$ are plotted in Figure 2.4, normalized by the corresponding values at $e = 10$.

For void ratios between 6 and 18 the variation of $G(e)$ with e seems to be acceptably small, see Figure 2.4. Taking G to be a constant, (2.43) can be written as

$$\frac{1}{G}\frac{\partial e}{\partial t} = g(\rho_s - \rho_f) \frac{\mathrm{d}}{\mathrm{d}e}\left(\frac{\mathrm{d}e}{\mathrm{d}\sigma'}\right) \frac{\partial e}{\partial z} + \frac{\partial^2 e}{\partial z^2}. \tag{2.47}$$

This equation is still non-linear due to the variable coefficient

$$\lambda(e) = -\frac{\mathrm{d}}{\mathrm{d}e}\left(\frac{\mathrm{d}e}{\mathrm{d}\sigma'}\right) \tag{2.48}$$

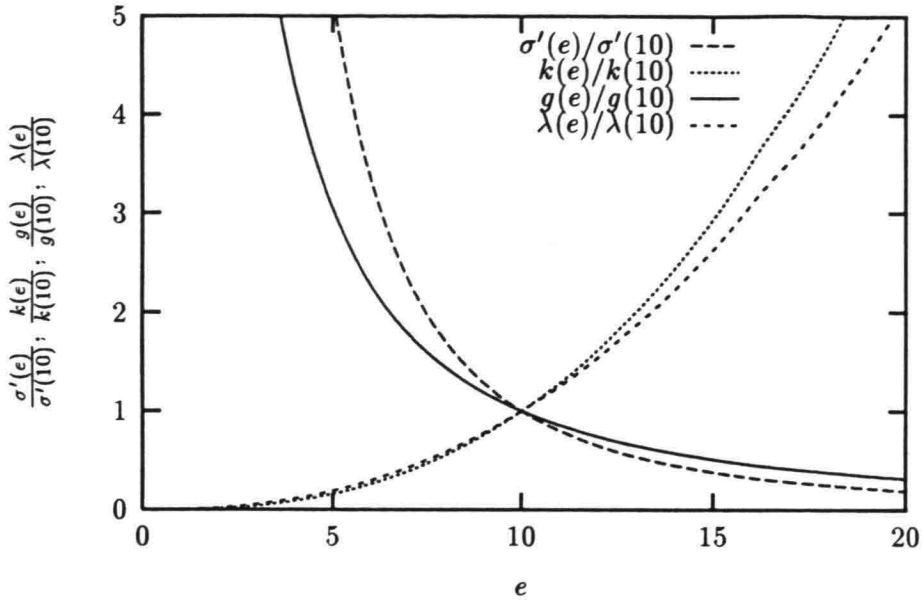

Figure 2.4: Sensitivity of the coefficient $G(e)$.

If λ is assumed to be a constant then (2.47) becomes a linear equation. However, this assumption seems to be acceptable for low void ratios only, see Figure 2.4.

In the case that λ is constant, (2.48) can be integrated with respect to e yielding

$$e = (e_0 - e_\infty)\exp(-\lambda\sigma') + e_\infty, \tag{2.49}$$

where e_0 is the void ratio for zero effective stress and e_∞ is the void ratio at the end of consolidation ($\sigma' \gg 0$).

The two-parameter relation (2.45) and the three-parameter relation (2.49) are plotted together with results from experiments with consolidating Combwich mud (Bowden, 1988) in Figure 2.5. In this figure the dotted line represents the two-parameter relation (2.45) and the solid line represents the three-parameter relation (2.49). The parameters used in the empirical relations are obtained by curve fitting and they are tabulated in Table 2.2. Notice that *specific volume* in Figure 2.5 is defined as $1 + e$.

Table 2.2: Empirical parameters fitted on results of experiments with Combwich mud (Bowden, 1988)

Two-parameter relation (2.45)				Three-parameter relation (2.49)			
A_p	=	12.800	(–)	e_0	=	7.422	(–)
B_p	=	0.153	(–)	e_∞	=	4.64	(–)
				λ	=	$4.811 \cdot 10^{-3}$	(Pa^{-1})

The correspondence between the experimental results and the empirical relations is quite good, see Figure 2.5. Only for high void ratios the three-parameter relation starts to deviate.

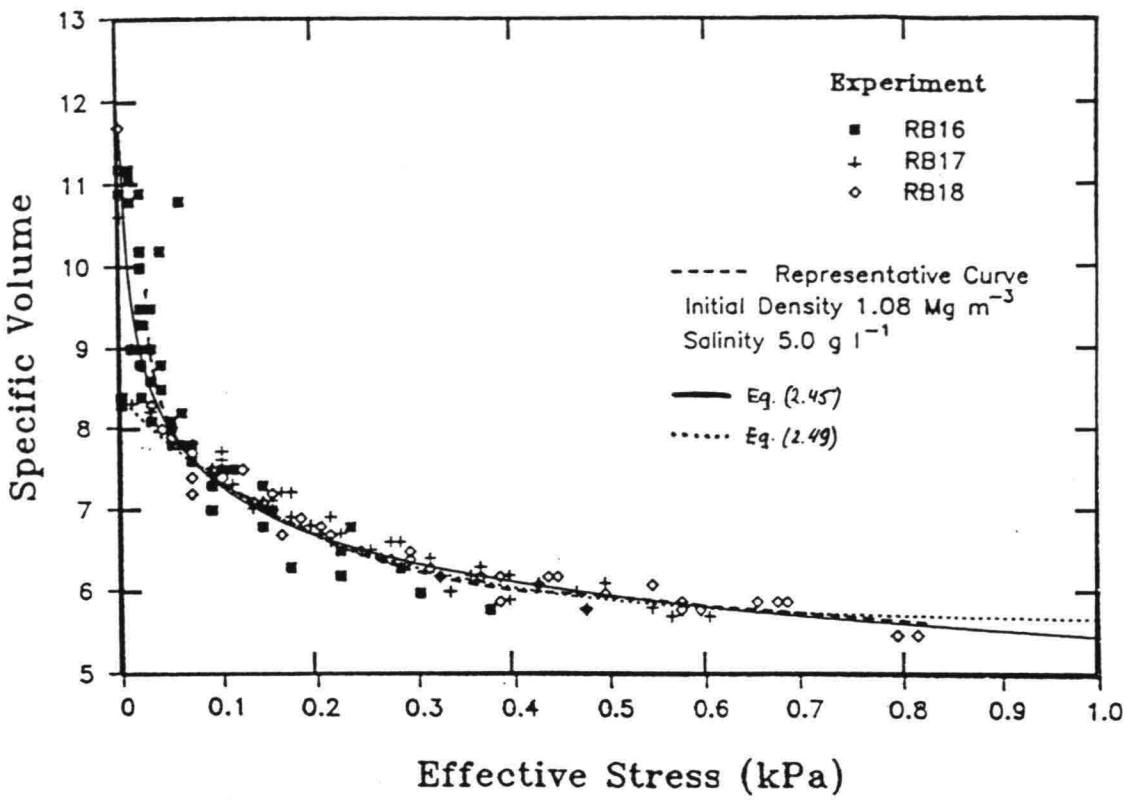

Figure 2.5: Empirical relations and results of experiments (Bowden, 1988)

This is to be expected, since for high void ratios the parameter λ, which is assumed to be constant, changes rapidly with e, see Figure 2.4.

It is noted that the results of experiment RB16, RB17 and RB18 are obtained from *one* experiment, but at different points of time, (Bowden, 1988). This explains the absence of extreme scatter usually found in $e - \sigma'$ plots.

2.4 Initial and boundary conditions

In order to solve Gibson's consolidation equation, two boundary conditions and one initial condition have to be specified. The problem considered here is consolidating mud in a column with either a pervious or an impervious base.

2.4.1 Initial conditions

The specification of the initial conditions is straightforward. The distribution of the void ratio at $t = 0$ defines the beginning situation:

$$e_{\text{ini}}(z) = e(z, 0). \tag{2.50}$$

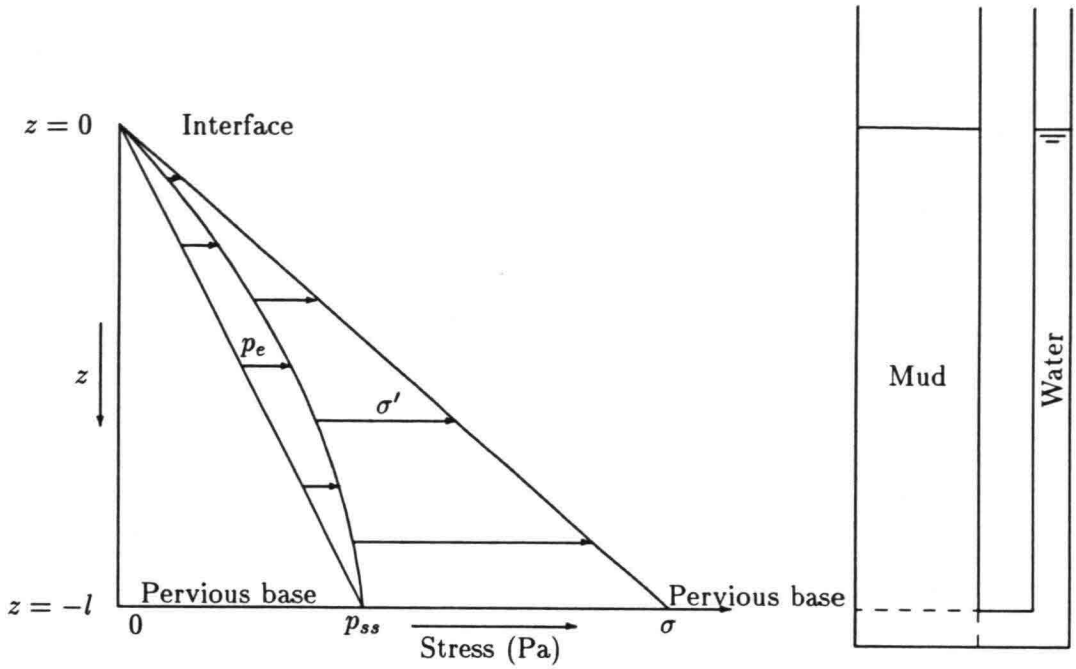

Figure 2.6: Stress distributions for consolidating mud in a column with a pervious base.

2.4.2 Boundary conditions

In Section 2.3 it was shown that the three-parameter relation (2.49), from the linearized Gibson equation (2.47), matches the experimental results of Bowden (1988) quite satisfactory. Since a relationship between σ' and e is necessary for the specification of the boundary conditions, (2.49) is used (Gibson *et al.*, 1981). However, other relations can be used as well.

The upper boundary condition: the interface

At the interface it is assumed that there is no effective stress. Substituting $\sigma' = 0$ into (2.49) yields

$$e_{\text{interface}} = e_0. \tag{2.51}$$

Changes in void ratio at the interface are not accounted for in this formulation. It may be expected that, when the consolidation process proceeds and thus the pore water flow decreases, the permeability decreases. Since the void ratio and the permeability are strongly related, the void ratio decreases during consolidation as well.

The lower boundary: pervious base

In Figure 2.6 the stress distributions are sketched of consolidating mud in a column with a pervious base.

Vertical equilibrium reads, in material coordinates,

$$\frac{\partial \sigma}{\partial z} = -e\rho_f g - \rho_s g. \tag{2.52}$$

This equation is obtained by transforming (2.2) to material coordinates according to (2.19). Differentiating the effective stress expression (2.11) with respect to z yields

$$\frac{\partial \sigma'}{\partial z} = \frac{\partial \sigma}{\partial z} - \frac{\partial p_{ss}}{\partial z} - \frac{\partial p_e}{\partial z}. \tag{2.53}$$

Substituting from (2.52), equation (2.53) yields after integration with respect to z

$$\sigma'(z) = -g(\rho_s - \rho_f)z - p_e(z). \tag{2.54}$$

As the base is pervious, the excess pore water pressure always equals zero at the base ($z = -l$), thus

$$\sigma'(-l, t) = g(\rho_s - \rho_f)l. \tag{2.55}$$

Combining (2.49) and (2.55) yields the lower boundary condition for a pervious base:

$$e(-l, t) = (e_0 - e_\infty)\exp(-\lambda g(\rho_s - \rho_f)l) + e_\infty. \tag{2.56}$$

The lower boundary condition: impervious base

Now the mud is consolidating in a column with an impervious base. At the base of the column $v_s = v_f = 0$. Substituting $v_s = 0$ into (2.10) yields

$$\frac{\partial p}{\partial x} = -\rho_f g, \tag{2.57}$$

so that at the base of the column

$$\frac{\partial p_e}{\partial x} = 0, \tag{2.58}$$

and thus

$$\frac{\partial p_e}{\partial z} = 0. \tag{2.59}$$

Combining (2.52), (2.53) and (2.59) gives

$$\frac{\partial \sigma'}{\partial z} + g(\rho_s - \rho_f) = 0 \Big|_{z=-l} \tag{2.60}$$

Again assuming that σ' is a function of the void ratio only, equation (2.60) can be written as

$$\frac{\partial e}{\partial z} + g(\rho_s - \rho_f)\frac{\mathrm{d}e}{\mathrm{d}\sigma'} = 0, \tag{2.61}$$

which is the boundary condition for an impervious base.

Chapter 3

Theory of rheology

In this chapter some principles of the use of tensors are presented. Subsequently a number of constitutive relations are described, starting with the simple model for Newtonian fluids. The models become increasingly more complex in order to describe more complex materials. The ultimate goal is a rheological model for describing the complex behaviour of mud.

3.1 Deformation and stress tensors

Any material that is subjected to stresses deforms. How and how much it deforms depends on material properties and the specific circumstances. This matter will be treated later. Consider a cubic element, which has been deformed as a result of an arbitrary load.

The deformation or strain can be written in tensor notation:

$$\boldsymbol{E} = \begin{bmatrix} \varepsilon_{xx} & \varepsilon_{xy} & \varepsilon_{xz} \\ \varepsilon_{yx} & \varepsilon_{yy} & \varepsilon_{yz} \\ \varepsilon_{zx} & \varepsilon_{zy} & \varepsilon_{zz} \end{bmatrix}. \tag{3.1}$$

The elements ε_{ij} are given by

$$\varepsilon_{ij} = \frac{1}{2}\left(\frac{\partial s_i}{\partial x_j} + \frac{\partial s_j}{\partial x_i}\right) \qquad \forall\,(i,j)\,\epsilon\{1,2,3\}, \tag{3.2}$$

where $\boldsymbol{s}$ is the displacement. Deformation can be decomposed into compression and distorsion. In contrast with distorsion, compression changes the volume of an element. For compression or volume strain we have

$$\varepsilon^* = \varepsilon_{xx} + \varepsilon_{yy} + \varepsilon_{zz}. \tag{3.3}$$

The deviatoric strain or distorsion is given by

$$\boldsymbol{E}_d = \begin{bmatrix} \varepsilon_{xx} - \frac{1}{3}\varepsilon^* & \varepsilon_{xy} & \varepsilon_{xz} \\ \varepsilon_{yx} & \varepsilon_{yy} - \frac{1}{3}\varepsilon^* & \varepsilon_{yz} \\ \varepsilon_{zx} & \varepsilon_{zy} & \varepsilon_{zz} - \frac{1}{3}\varepsilon^* \end{bmatrix}. \tag{3.4}$$

When flowing materials are considered, it is more convenient to describe strain rates rather than just strain, although both strain and strain rate play a role in the case of visco-elastic materials. The strain rate tensor is given by

$$\boldsymbol{D} = \frac{\partial}{\partial t}\boldsymbol{E} = \begin{bmatrix} \dot{\varepsilon}_{xx} & \dot{\varepsilon}_{xy} & \dot{\varepsilon}_{xz} \\ \dot{\varepsilon}_{yx} & \dot{\varepsilon}_{yy} & \dot{\varepsilon}_{yz} \\ \dot{\varepsilon}_{zx} & \dot{\varepsilon}_{zy} & \dot{\varepsilon}_{zz} \end{bmatrix}, \tag{3.5}$$

where the elements $\dot{\varepsilon}_{ij}$ are given by

$$\dot{\varepsilon}_{ij} = \frac{1}{2}\left(\frac{\partial u_i}{\partial x_j} + \frac{\partial u_j}{\partial x_i}\right) \qquad \forall\,(i,j)\,\epsilon\{1,2,3\}, \tag{3.6}$$

where $\boldsymbol{u}$ is the local velocity.

The deviatoric strain rate tensor is given by

$$\boldsymbol{D}_d = \begin{bmatrix} \dot{\varepsilon}_{xx} - \frac{1}{3}\dot{\varepsilon}^* & \dot{\varepsilon}_{xy} & \dot{\varepsilon}_{xz} \\ \dot{\varepsilon}_{yx} & \dot{\varepsilon}_{yy} - \frac{1}{3}\dot{\varepsilon}^* & \dot{\varepsilon}_{yz} \\ \dot{\varepsilon}_{zx} & \dot{\varepsilon}_{zy} & \dot{\varepsilon}_{zz} - \frac{1}{3}\dot{\varepsilon}^* \end{bmatrix}. \tag{3.7}$$

Stresses can be written in tensor notation as well. The stress tensor reads

$$\boldsymbol{S} = \begin{bmatrix} \sigma_{xx} & \sigma_{xy} & \sigma_{xz} \\ \sigma_{yx} & \sigma_{yy} & \sigma_{yz} \\ \sigma_{zx} & \sigma_{zy} & \sigma_{zz} \end{bmatrix}. \tag{3.8}$$

As with strains, stresses are decomposed into compressive stresses and distorsive stresses. The compressive stress is defined as

$$\sigma_0 = \frac{1}{3}(\sigma_{xx} + \sigma_{yy} + \sigma_{zz}). \tag{3.9}$$

The isotropic stress σ_0 is the averaged normal stress.

The deviatoric stresses are given by the tensor

$$\boldsymbol{S}_d = \begin{bmatrix} \sigma_{xx} - \sigma_0 & \sigma_{xy} & \sigma_{xz} \\ \sigma_{yx} & \sigma_{yy} - \sigma_0 & \sigma_{yz} \\ \sigma_{zx} & \sigma_{zy} & \sigma_{zz} - \sigma_0 \end{bmatrix}. \tag{3.10}$$

Simplification by assuming incompressibility

In the case that the fluid is considered to be incompressible, the stress and strain tensors simplify because the volumetric strain vanishes,

$$\varepsilon^* = \varepsilon_{xx} + \varepsilon_{yy} + \varepsilon_{zz} = 0. \tag{3.11}$$

With this condition the strain tensor $\boldsymbol{E}$ equals the deviatoric strain tensor $\boldsymbol{E}_d$, and similarly, the strain rate tensor $\boldsymbol{D}$ equals the deviatoric strain rate tensor $\boldsymbol{D}_d$.

Invariants of a tensor

Tensors used within this context describe strain (rate) or stress at an arbitrary point within the mud layer. The magnitude and sign of the tensor elements depend on the spatial orientation of the (orthogonal) coordinate system[1]. However, the state at the point under consideration is independent of the orientation of the coordinate system. A property of tensors is that they have some special combinations of their elements (invariants), which values are independent of the orientation of the coordinate system.

Let $\boldsymbol{T}$ be a second order tensor, describing either strain (rate) or stress, then $\boldsymbol{T}$ has three invariants[2]:

$$\mathrm{I}_{\boldsymbol{T}} = \mathrm{trace}(\boldsymbol{T}) \tag{3.12}$$

$$\mathrm{II}_{\boldsymbol{T}} = \boldsymbol{T} : \boldsymbol{T} \tag{3.13}$$

$$\mathrm{III}_{\boldsymbol{T}} = \det(\boldsymbol{T}) \tag{3.14}$$

The values of these invariants provide information about the local state of the material regardless how the carthesian coordinate system is chosen. They may be used as parameters in constitutive relations.

3.2 Constitutive relations

The stress and strain (rate) constitution in an arbitrary point within a soil layer is described by the tensors given in the previous section. Viscosity relates stresses to deformations and *vice versa*. The viscosity of a material may depend on many factors. The most important factor is the material (composition) itself. Further temperature, history and the nature and magnitude of deformation may play a role. In order to describe the relation between stresses and deformations (empirical) models can be formulated. The search for appropriate constitutive models for fluids is the task of rheology.

With respect to viscous behaviour fluids can be classified as follows:

- Fluids of Pascal
- Newtonian fluids
- Non-Newtonian fluids

A Pascalian fluid is inviscid. As a result such a fluid is not subjected to internal friction, and thus no momentum can be transferred. Therefore this type of fluids is irrelevant with respect to rheology.

A Newtonian fluid is an idealized fluid. The viscosity is a material function that is independent of the deformation (rate) and history of the material, but may vary with temperature and possibly pressure. In practice water is most modelled adequately as a Newtonian fluid.

Fluids that have a more complicated behaviour are classified as non-Newtonian fluids. This group can be divided in many subdivisions. This will be discussed later.

[1] Unless stated otherwise, all phenomena are described in a cartesian (orthogonal) coordinate system.
[2] See also Appendix B.

3.2.1 Constitutive model for Newtonian fluids

The constitutive model for a Newtonian fluid is given by (Bird *et al.*, 1960)

$$\boldsymbol{S} = -\left[(\kappa + \frac{2}{3}\eta)\nabla \cdot \boldsymbol{u}\right]\boldsymbol{I} + 2\eta\boldsymbol{D}, \tag{3.15}$$

where η is the viscosity, κ is the dynamic bulk viscosity or dynamic bulk modulus and $\boldsymbol{I}$ is the unity tensor.

Equation (3.15) can be rewritten by subtracting the normal components

$$\sigma_0 \boldsymbol{I} = -(\kappa\nabla \cdot \boldsymbol{u})\boldsymbol{I} \tag{3.16}$$

yielding

$$\boldsymbol{S}_d = -(\frac{2}{3}\eta\nabla \cdot \boldsymbol{u})\boldsymbol{I} + 2\eta\boldsymbol{D}. \tag{3.17}$$

Notice that, if (3.17) is written in the deviatoric strain rate $\boldsymbol{D}_d$, then the first term of the right-hand side vanishes:

$$\boldsymbol{S}_d = 2\eta\boldsymbol{D}_d \tag{3.18}$$

The magnitude of the dynamic bulk viscosity is material and process dependent. For rarefied gases κ approaches zero. For dense gases and even fluids the dynamic bulk viscosity is probably not too important (Bird *et al.*, 1960). Moreover, in the consolidation theory the incompressibility assumption $(\nabla \cdot \boldsymbol{u})$ is used. The incompressibility assumption reduces the stress–strain rate relation to the deviatoric part.

Flow curves

The relation between stress and strain rate is often presented graphically in a so-called flow curve. In order to plot the results of a mathematical model it is convenient to rewrite the mathematical model in terms of invariants. The most appropriate invariant is the second, since the first invariant equals zero if incompressibility is assumed and the third invariant is equal to zero for various viscometric flows, such as axial tube flow, axial and tangential annular flow and flow in a film.

Equation (3.18), written in terms of second invariants, reads

$$\mathrm{II}_{\boldsymbol{S}_d} = 4\eta^2 \mathrm{II}_{\boldsymbol{D}_d} \tag{3.19}$$

Plotting this equation in $(\mathrm{II}_{\boldsymbol{D}_d}, \mathrm{II}_{\boldsymbol{S}_d})$ space is not convenient, since most flow curves are obtained from viscometric flow conditions and consequently plotted in $(\tau_{yx}, \dot{\gamma})$ space. For viscometric flow the strain rate $\dot{\gamma}$ is defined by

$$\dot{\gamma} = \frac{\partial u}{\partial y}, \tag{3.20}$$

where u represents the x-component of the velocity $\boldsymbol{u}$, and y is a coordinate normal to the x-coordinate. For viscometric flow conditions the following relations hold:

$$\dot{\gamma} = 2\sqrt{\tfrac{1}{2}\mathrm{II}_{\boldsymbol{D}_d}} = \sqrt{2\mathrm{II}_{\boldsymbol{D}_d}}, \tag{3.21}$$

$$\tau_{yx} = \sqrt{\tfrac{1}{2}\mathrm{II}_{\boldsymbol{S}_d}}. \tag{3.22}$$

Correspondingly (3.19) is written as [3]

$$\sqrt{\tfrac{1}{2}\mathrm{II}_{S_d}} = 2\eta\sqrt{\tfrac{1}{2}\mathrm{II}_{D_d}}, \tag{3.23}$$

and plotted in $(2\sqrt{\frac{1}{2}\mathrm{II}_{D_d}}, \sqrt{\frac{1}{2}\mathrm{II}_{S_d}})$ space.

For Newtonian fluids, modelled by (3.18), the flow curve is a straight line through the origin, see Figure 3.1.

3.2.2 Constitutive models for non-Newtonian fluids

Fluids that do not obey Newton's viscosity model are called non-Newtonian fluids. These fluids can be classified into three subdivisions (Van Rijn, 1990):

- fluids for which the shear stress depends only on the shear rate, and although the relation between them is not linear, it is independent of the time the fluid has been sheared,
- fluids for which the shear stress depends not only on the shear rate, but also on the time the fluid has been sheared or its history, and
- visco-elastic fluids which exhibit characteristics of both elastic solids and viscous fluids.

The first group can be characterized as the most simple form of non-Newtonian fluids. Now, the viscosity η is dependent on strain rate as well. Objective information about strain rate is obtained via the three strain rate tensor invariants introduced earlier. Hence, the $\boldsymbol{S} - \boldsymbol{D}$ relation becomes

$$\boldsymbol{S} = -\left[(\kappa + \frac{2}{3}\eta)\nabla \cdot \boldsymbol{u}\right] \boldsymbol{I} + 2\eta \boldsymbol{D}, \tag{3.24}$$

where

$$\eta = \eta(\mathrm{I}_{\boldsymbol{D}}, \mathrm{II}_{\boldsymbol{D}}, \mathrm{III}_{\boldsymbol{D}}). \tag{3.25}$$

From this point attention is paid to the deviatoric part of (3.24) only. If it is justified to assume incompressibility, which is the case for saturated soils, the deviatoric part of the stress–strain rate relation provides sufficient information to compute the stress-strain rate behaviour of the fluid, otherwise the normal component has to be taken in account (separately) as well, including the dynamic bulk viscosity.

The deviatoric component of (3.24) reads

$$\boldsymbol{S}_d = -2\eta(\mathrm{II}_{\boldsymbol{D}_d}, \mathrm{III}_{\boldsymbol{D}_d})\boldsymbol{D}_d. \tag{3.26}$$

The first invariant of $\boldsymbol{D}_d$ represents the volumetric strain rate of distorsion, which is equal to zero by definition. Hence, the first invariant does not appear in (3.26). In many models

[3] In this form only the first quadrant is accounted for. The correct formulation would be $\sqrt{\frac{1}{2}\mathrm{II}_{S_d}} = \pm 2\eta\sqrt{\frac{1}{2}\mathrm{II}_{D_d}}$.

found in the literature, the viscosity is only a function of the second invariant. Probably, the influence of the third invariant is not understood, or considered to be of minor importance (Bird *et al.*, 1960). Moreover, in viscometric flow $\mathrm{III}_{\boldsymbol{D}_d} = 0$. Consequently, the models, found in the literature, are generally written with η as function of the second invariant of $\boldsymbol{D}_d$:

$$\boldsymbol{S}_d = 2\eta(\mathrm{II}_{\boldsymbol{D}_d})\boldsymbol{D}_d. \tag{3.27}$$

Below some models based on the concept of (3.27) are discussed briefly.

Bingham model

The two-parameter (η_0, τ_0) Bingham model extends the Newtonian model by introducing a yield stress τ_0. As long as the applied shear stresses are smaller than the yield stress, no deformation occurs. The mathematical expression for the Bingham model reads

$$\boldsymbol{S}_d = 2\left[\eta_0 + \frac{\tau_0}{\sqrt{2\mathrm{II}_{\boldsymbol{D}_d}}}\right]\boldsymbol{D}_d, \qquad \boldsymbol{D}_d = 0 \;\forall\; \frac{1}{2}\mathrm{II}_{\boldsymbol{S}_d} < \tau_0^2 \tag{3.28}$$

It can be shown that, given a stress situation, the shear stress acting on the maximally sheared plane equals $\sqrt{\frac{1}{2}\mathrm{II}_{\boldsymbol{S}_d}}$, which explains the yielding conditioning.

Ostwald–de Waele model (powerlaw)

The two-parameter (η_0, n) Ostwald–de Waele model, sometimes referred to as the power law model, is able to describe dilatant behaviour, i.e. increasing viscosity with increasing strain rate, and pseudoplastic behaviour, which the opposite of dilatancy. The model incorporates no yield stress. The mathematical formulation reads

$$\boldsymbol{S}_d = 2\left[\eta_0\sqrt{2\mathrm{II}_{\boldsymbol{D}_d}}^{(n-1)}\right]\boldsymbol{D}_d. \tag{3.29}$$

Setting $n = 1$, the power law reduces to Newton's law of viscosity. For n greater than unity, the behaviour is dilatant (shear thinning), whereas for values less than unity the behaviour is pseudoplastic.

Reiner–Philippoff model

This model contains three adjustable parameters: η_0, η_∞ and τ_0. Since Newtonian behaviour has often been observed both at very low and very high strain rates, the model has been set up to reduce to Newton's law of viscosity with $\eta = \eta_0$ and $\eta = \eta_\infty$, respectively, for these two limiting cases. The mathematical formulation of the Reiner–Philippoff model reads

$$\boldsymbol{S}_d = 2\left[\eta_\infty + \frac{\eta_0 - \eta_\infty}{1 + \frac{\frac{1}{2}\mathrm{II}_{\boldsymbol{S}_d}}{\tau_0^2}}\right]\boldsymbol{D}_d. \tag{3.30}$$

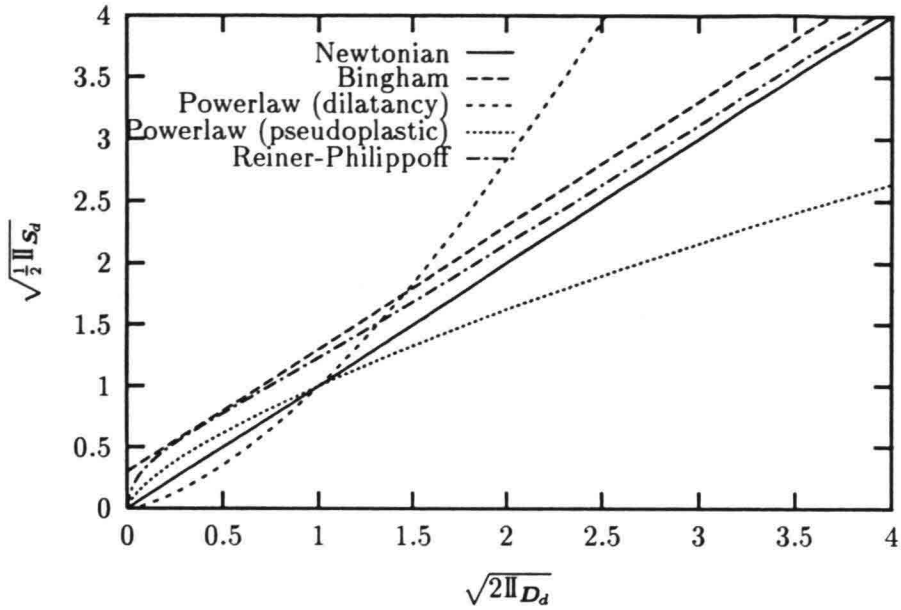

Figure 3.1: Flow curves (qualitatively)

At moderate strain rates the behaviour changes from pseudoplastic into dilatant with increasing strain rates and for $\eta_0 > \eta_\infty$. The coordinates of the inflection point are

$$(\mathrm{II}_{D_d}, \mathrm{II}_{S_d}) = \left(\frac{3}{32} \frac{(\eta_\infty + 3\eta_0)^2 \tau_0^2}{\eta_\infty^3 \eta_0}, 6\tau_0^2 \frac{\eta_0}{\eta_\infty} \right), \tag{3.31}$$

see also Appendix A.

If the viscosity at low strain rates is very high, then the Reiner-Philippoff model can be considered as the continuous form of the Bingham model. Then $(\frac{1}{2}\mathrm{II}_{S_d})^{\frac{1}{2}}_{\text{inflection}} = \tau_0\sqrt{3\eta_0/\eta_\infty}$ corresponds to the Bingham yield stress.

3.2.3 Constitutive models for non-Newtonian fluids including thixotropy

The viscosity in the models discussed so far is not time dependent. It has been observed that some materials are thinning or thickening during deformation. Various types of this rheological phenomena can be discerned:

- Thixotropy, defined as the decrease in viscosity under stress, followed by gradual recovery when the stress is removed.
- Anti-thixotropy, the opposite of thixotropy.
- Rheopexy, defined as the acceleration of solidification of a material by gentle regular movements. The material has an enhanced rate of recovery at low shear rates compared with that at rest. Sometimes the notion rheopexy is incorrectly used as synonymous to anti-thixotropy.

- Partial thixotropy, defined as partially irreversible thixotropy. Materials that do not recover at all, are called rheomalaxis.

The cause of time dependent behaviour has to be sought in changes in the structure of the fluid at microscale. In a dispersion for example, the structural formation is due to interparticle forces acting between the dispersed species in the fluid. The forces involved are Van der Waals' forces and forces generated by electric interaction, double layers (Olphen & Fripiat, 1979) and steric interaction.

Depending on the interplay of attraction and repulsion, flocs of different sizes, shapes and strengths may be formed. The viscosity depends on the floc size and shape among other things. The rate of formation and destruction of flocs is governed by Brownian motion and shear. A material shows thixotropic behaviour if the internal structure is built up in rest and broken up by shear.

The modelling of thixotropic behaviour requires knowledge of interparticle forces and internal structures. Many different microscopic processes may result in time dependent behaviour. In the literature some theoretical models can be found, dealing with one aspect causing the thixotropy. A comprehensive thixotropic model would have to account for many factors, which is a complicated undertaking.

Lumped parameter models

In another, more global, approach to thixotropic modelling, the details of the structure, i.e. concentration, shape and size distribution, and its internal constitution, are replaced by a structure parameter λ. The viscosity is evaluated in terms of λ and the time dependent behaviour is described by a rate equation for λ.

The parameter λ quantifies the degree of structural formation. When the fluid is fully built up, λ equals unity and when the fluid is fully broken up, λ equals zero. In the initial (undisturbed) state $\lambda = \lambda_0$, where λ_0 is often taken equal to unity. However, Worrall and Tuliani (1964), who studied the effect of aging on the rheology of clay suspensions, state that λ approaches unity rather than that it reaches unity. Hence, $\lambda = 1$ refers to the maximal possible structure measured during testing the sample, and not the maximal possible structure the sample ever can get.

The parameter λ is a measure for structure, and hence, the structural parameter may be related to the strength or yield stress. Billington (1960) proposed the following definition:

$$\lambda(t) = \frac{\tau_y(t) - \tau_\infty}{\tau_0 - \tau_\infty}, \tag{3.32}$$

where τ_0 refers to the yield stress at $t = 0$ and τ_∞ refers to the yield stress for shear rates approaching infinity. Since Newtonian behaviour is often observed for high shear rates, τ_∞ is assumed to be zero, so that (3.32) reduces to

$$\lambda(t) = \frac{\tau_y(t)}{\tau_0}. \tag{3.33}$$

$\eta = \eta_0 + \eta_1 \lambda$

$0 \leq \lambda \leq 1$

$\frac{d\lambda}{dt} = a(1-\lambda) - b\lambda\dot{\gamma}$

Moore model

The simplest lumped parameter model is the Moore model (Moore, 1959). He postulated that the viscosity of the thixotropic fluid can be described by

$$\eta = \eta_\infty + c\lambda, \qquad \lambda \in [0,1]. \tag{3.34}$$

The constitutive equation is then

$$\boldsymbol{S}_d = 2(\eta_\infty + c\lambda)\boldsymbol{D}_d. \tag{3.35}$$

The rate equation for λ is given by

$$\frac{\mathrm{d}\lambda}{\mathrm{d}t} = a(1-\lambda) - b\lambda\sqrt{2\mathrm{II}_{\boldsymbol{D}_d}}. \tag{3.36}$$

The first term of the right-hand side of (3.36) quantifies the build-up rate. It is assumed that the build-up rate of the fluid depends on the amount of structure to be recovered $(1-\lambda)$. The second term of the right-hand side quantifies the break up rate, which is assumed to depend on both the shear rate $\sqrt{2\mathrm{II}_{\boldsymbol{D}_d}}$ and the current structure λ.

The equilibrium value, λ_e, of the structural parameter λ_e follows from $\mathrm{d}\lambda/\mathrm{d}t = 0$, which gives

$$\lambda_e = \frac{a}{a + b\sqrt{2\mathrm{II}_{\boldsymbol{D}_d}}} = \frac{1}{1 + \beta\sqrt{2\mathrm{II}_{\boldsymbol{D}_d}}}, \tag{3.37}$$

where $\beta = b/a$.

Worrall and Tuliani model

Worrall and Tuliani (1964) combined the Moore model for equilibrium and the Bingham model:

$$\boldsymbol{S}_d = 2\left(\frac{\lambda_0\tau_0}{\sqrt{2\mathrm{II}_{\boldsymbol{D}_d}}} + \mu_\infty + c\lambda_e\right)\boldsymbol{D}_d, \qquad \boldsymbol{D}_d = 0 \;\forall\; \frac{1}{2}\mathrm{II}_{\boldsymbol{S}_d} < \tau_0^2 \tag{3.38}$$

This model describes the behaviour in state of equilibrium of thixotropic materials that have a yield stress.

Toorman model

Toorman (1995) proposed a new rheological equation. He generalizes (3.38) by postulating that all rheological parameters can be a function of λ:

$$\boldsymbol{S}_d = 2\left(\frac{\tau_y(\lambda)}{\sqrt{2\mathrm{II}_{\boldsymbol{D}_d}}} + \mu(\sqrt{2\mathrm{II}_{\boldsymbol{D}_d}}, \lambda)\right)\boldsymbol{D}_d, \tag{3.39}$$

which is rewritten after substitution of (3.33) as

$$\boldsymbol{S}_d = 2\left(\lambda\frac{\tau_0}{\sqrt{2\mathrm{II}_{\boldsymbol{D}_d}}} + \eta_\infty(\sqrt{2\mathrm{II}_{\boldsymbol{D}_d}}) + c\lambda\right)\boldsymbol{D}_d, \tag{3.40}$$

For the state of equilibrium (3.40) gives

$$\boldsymbol{S}_d = 2\left(\lambda_e \frac{\tau_0}{\sqrt{2\mathrm{II}_{\boldsymbol{D}_d}}} + \eta_\infty(\sqrt{2\mathrm{II}_{\boldsymbol{D}_d}}) + c\lambda_e\right)\boldsymbol{D}_d, \tag{3.41}$$

which corresponds to the Worrall and Tuliani model (3.38). Equating these two formulations yields the relationship:

$$(\lambda_0 - \lambda_e)\frac{\tau_0}{\sqrt{2\mathrm{II}_{\boldsymbol{D}_d}}} + \mu_\infty - \eta_\infty(\sqrt{2\mathrm{II}_{\boldsymbol{D}_d}}) = 0. \tag{3.42}$$

Substitution of (3.42) into (3.41) yields

$$\boldsymbol{S}_d = 2\left((\lambda_0 + \lambda - \lambda_e)\frac{\tau_0}{\sqrt{2\mathrm{II}_{\boldsymbol{D}_d}}} + \mu_\infty + c\lambda\right)\boldsymbol{D}_d. \tag{3.43}$$

Equation (3.43) is the new rheological model, expressed in equilibrium flow curve (EFC) parameters, for a thixotropic yield stress fluid, proposed by Toorman (1995). Notice that so far no constraints have been made on the rate equation.

Super-structure

If the internal structure of the material does not change, the relation between deformation rate and stress, and stress and deformation rate is unique. Consequently, the relation between deformation rate and stress must be either monotonic ascending or monotonic descending. Since at large deformation rates the stress increases with increasing deformation rates, the relation is monotonic ascending, or in other words, the differential viscosity must always be non-negative. However, during shearing experiments it is often observed that at low shear rates the stress drops to a lower value when shear rate increases, resulting in a flow curve with a stress minimum, see Figure 3.2. This effect can only be explained by a changing internal structure.

Cheng (1986) distinguishes between two yield stresses. The yield stress pertaining to the equilibrium flow curve is called the dynamic yield stress τ_d (short time scale), whereas the yield stress measured after a long storage is called the static yield stress τ_s (long time scale). For simple thixotropic fluids the static yield stress equals the dynamic yield stress, but for many materials including mud, the static yield stress is generally larger than the dynamic yield stress.

A physical explanation is that the material in rest builds up a secondary structure. The formation of this structure is usually a slow process, but the structure rapidly breaks up when shear is applied. The existence of the second structure or super-structure in mud and clay suspensions may be related to coagulation and bacterial gluing.

The super-structure can be modelled by the introduction of a second structural parameter λ_s (Toorman, 1995). The thixotropic model (3.43) is modified by adding a term accounting for the super-structure:

$$\boldsymbol{S}_d = 2\left(\frac{\lambda_s(\tau_s - \tau_d) + (\lambda_0 + \lambda - \lambda_e)\tau_d}{\sqrt{2\mathrm{II}_{\boldsymbol{D}_d}}} + \mu_\infty + c\lambda\right)\boldsymbol{D}_d. \tag{3.44}$$

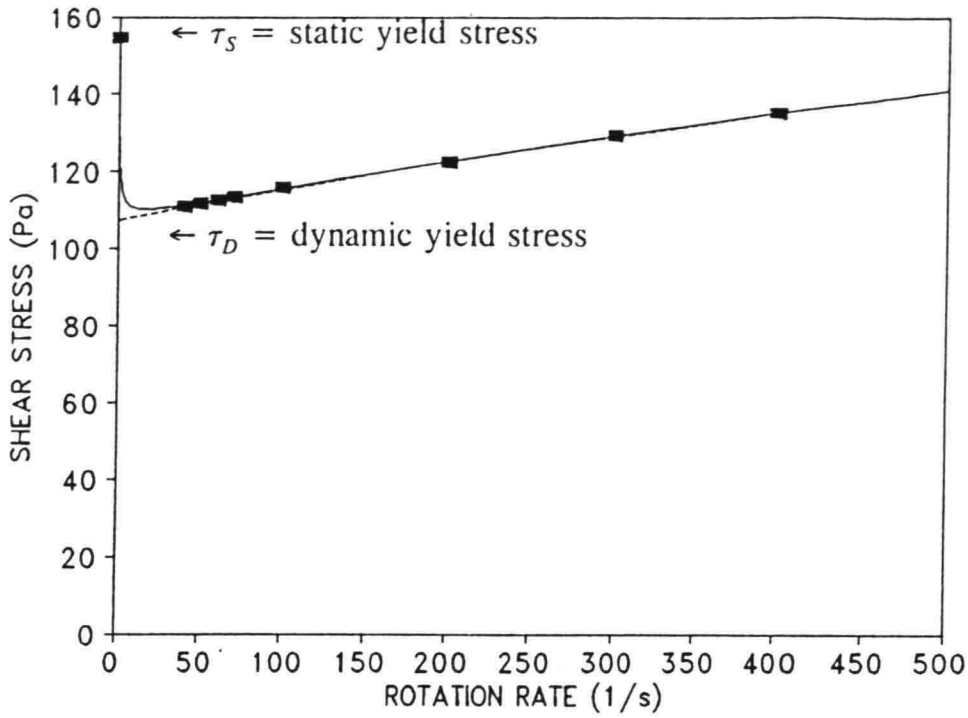

Figure 3.2: Static and dynamic yield stress for the equilibrium flow curve of a 4% aqueous bentonite suspension. Symbols=experimental data (Coussot *et al.*, 1993). Figure taken from (Toorman, 1995)

The rate equation for λ_s may be of the same form as that of λ (3.36). Consequently, the model will be harder to calibrate, since three more parameters (λ_s, a_s, b_s) have to be determined. But the model is able to reproduce the minimum in the flow curve (Toorman, 1995).

Chapter 4

Discussion and conclusions

The consolidation equation contains two material dependent parameters, namely the hydraulic conductivity k and the effective stress σ'. Gibson *et al.* (1967) assumed that both parameters depend on the void ratio only. However, many experiments proved that the assumption is not satisfactory (Been, 1980; Bowden, 1988).

When a mud layer is consolidating, the structure is too weak to carry the imposed load, so that its structure is collapsing continuously and therefore shows a fluid-like behaviour. Hence, the strength of a mud layer, relative to the effective stress, governs the consolidation process. Studying the rheological properties of the mud layer may result in a better modelling of the consolidation process.

4.1 Yield stress versus effective stress

Been (1980) performed some experiments with consolidating mud and two of his conclusions are that for void ratio's larger than approximately 6, the soil can have a range of effective stress from 0–100 Pa and that zero effective stress at the soil surface can occur with a wide range of void ratio's, but the spread of the values of the void ratio reduces significantly as the effective stress increases.

In the Chapter 3 some rheological models have been discussed. The more sophisticated models incorporate thixotropy and yield stress. Bowden (1988) studied experimentally the relation between yield stress and effective stress. The behaviour of various compositions of mud and saline water was investigated in settling columns. At various time points and levels within the soft soil, both effective stress and yield stress were measured. The effective stress was calculated by subtracting the pore water pressure from the total stress. The yield stress is measured with a vane apparatus. The conclusions from these experiments are that there is a remarkable linear relationship between yield stress and effective stress, see Figure 4.1. The slope of the straight line depends on the material composition. From this figure it can be seen that the straight line interpolation intersects the positive yield stress axis, which suggests that at zero effective stress the soil has a shear strength. This shear strength is commonly called true cohesion. From Bowden's (1988) experiments it is also found that both the yield stress and the true cohesion increase with time, however this effect is more effective for lower

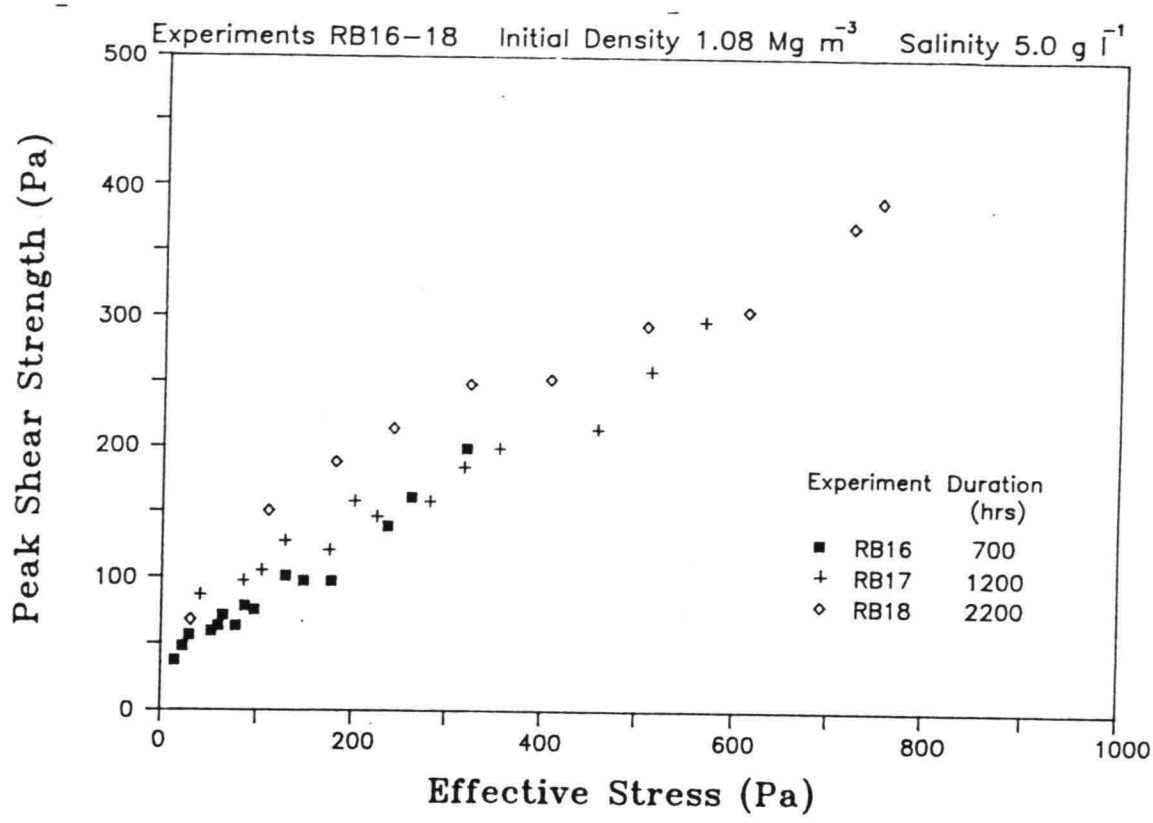

Figure 4.1: Yield stress versus effective stress. After (Bowden, 1988).

effective stress levels.

Van Kessel (1996) determined the yield strength of a consolidated bed of Caland mud by means of a sounding test. In this experiment a geometry penetrates into the bed while the bed is traversed upward, see Figure 4.2. The force acting on the geometry is recorded by a balance.

From the recorded forces the cohesion c of the bed are calculated, taking into account the contributions of the stresses at the tip of the geometry, the shear stress along the shaft, and the shape of the geometry, see (Van Kessel, 1996) for details. The cohesion c relates to the yield stress as

$$\tau_y = c + \sigma_n \tan(\phi), \tag{4.1}$$

where σ_n is the normal stress and ϕ is the angle of internal friction. For undrained experiments ϕ equals zero, so that (4.1) reduces to

$$\tau_y = c \tag{4.2}$$

Before the sounding test was executed, the density profile was determined with a conductivity probe. The effective stresses are calculated from the density profile. In Figure 4.3 the effective stress, here denoted by $\sigma_{v,0}$, is plotted as function of the yield stress, for various traversing speeds.

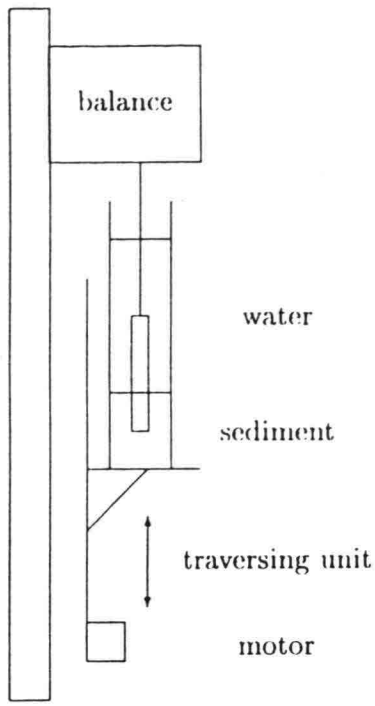

Figure 4.2: Experimental set-up (Van Kessel, 1996)

The traversing speed is quite important for the relation between yield stress and effective stress, see Figure 4.3. Only for relatively high traversing speeds, in this case 0.5 mm/s, the pore water cannot escape, resulting in an undrained condition. The plots for other traversing speeds correspond to (partial) drained conditions and are not considered here.

A continuous increase in effective stress with increasing yield stress can be observed. However, the relationship is not as linear as found by Bowden (1988), although the plot of results follows the line $\tau_y = \frac{1}{2}\sigma_{v,0}$ quite well. This line follows from Mohr's circle and indicates the (theoretical) maximum shear stress that can occur given the effective stress.

4.2 Topics for future research

Bowden (1988) and Van Kessel (1996) presented experimental evidence of a relationship between the effective stress and the yield stress. Because of the assumption that the effective stress and the permeability are a function of the void ratio only, aging, history effects, formation and break up of flocs, channeling and creep are neglected. In order to incorporate these effects into a consolidation model, a rheological model, that is to be implemented in such a consolidation model, has to be developed. To achieve this, the following items will be paid attention to:

- Set-up of an experimental programme,

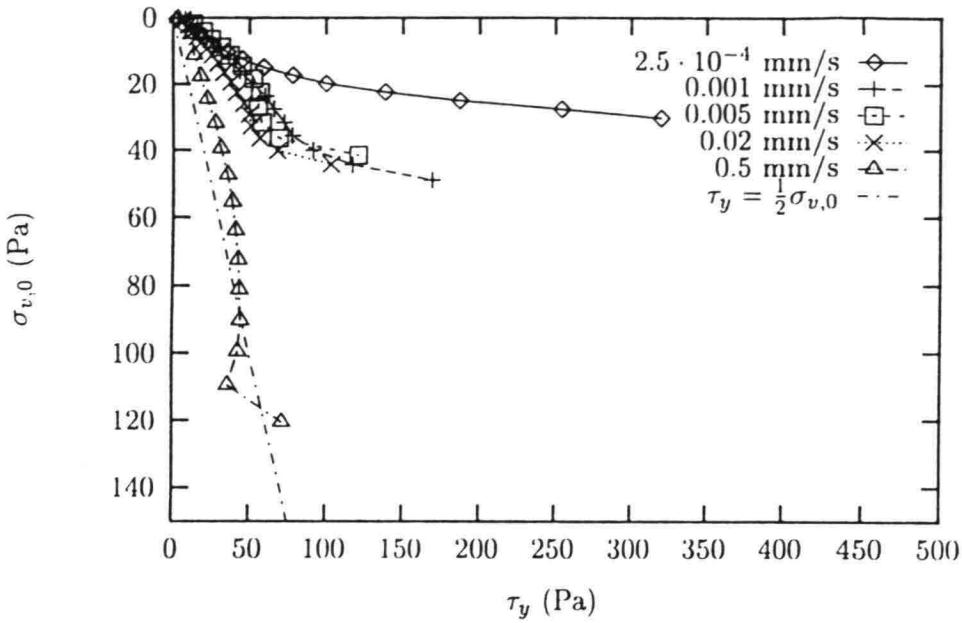

Figure 4.3: Yield strength versus initial vertical effective stress for Caland channel mud (Van Kessel, 1996)

- Development of an effective stress relation, based on the void ratio and rheological parameters,
- Development of an permeability relation, based on the void ratio and rheological parameters,
- Solving the one-dimensional consolidation model

4.3 Conclusions

Consolidation

A one-dimensional non-linear finite strain self-weight consolidation equation is presented in Eulerian coordinates. This equation is equivalent to Gibson's equation (1967) in Lagrangian-like material coordinates. It is shown that both Kynch's sedimentation theory (1952) and Terzaghi's consolidation theory (1943) are special cases of the Gibson equation.

Pane and Schiffman (1985) generalized the effective stress concept in order to link the sedimentation phase to the consolidation phase. However, generalized forms of the effective stress principle, derived by taking into account a small compressibility of the pore fluid and the particles, have a reduction factor multiplying the pore water pressure (Verruijt, 1984), whereas Pane and Schiffman used the factor multiplying the effective stress. Moreover, it is likely that in the intermediate region Terzaghi's effective principle is valid.

The solution of the consolidation equation requires, besides boundary conditions, two closure relations for the effective stress and the permeability. The relation between the effective stress and the void ratio is considered in some detail, whereas the relation for the permeability is left for a later discussion.

A relation for the effective stress is found from the linearized Gibson equation. This relation is compared with another commonly used empirical relation, see (Hu, 1990, for example), and experimental results with consolidating mud (Bowden, 1988). The correspondence is quite good.

In order to specify boundary conditions a relationship between the void ratio and the effective stress is needed. The boundary conditions for the interface, a pervious base and an impervious base are given.

Rheology

Rheological models describe the relationship between stress and strain (rate). Starting with simple rheological models, increasingly complex models to describe rheological complex fluids as mud are discussed.

Special attention has been paid to the modelling of fluids that show time dependent behaviour (thixotropy) and have a yield stress. The Toorman model (Toorman, 1995), which is a generalization of the Worrall and Tuliani model (Worrall & Tuliani, 1964), is presented. This model incorporates two yield stresses: a dynamic yield stress and a static yield stress, which is generally larger than the dynamic yield stress. The static yield stress represents a so-called super-structure that breaks up easily under shear, and builds up slowly in the absence of shear stresses. This model is able to represent the minima, that are often found in flow curves.

Bowden (1988) and Van Kessel (1996) presented experimental evidence of a relationship between the effective stress and the yield stress. This indicates that the incorporation of a rheological model into a consolidation model can result in a better modelling of the consolidation process.

Chapter 5

Acknowledgements

This literature survey is the first result of the Ph.D. project *Strength evolution of soft consolidating mud layers* which is financed by Netherlands Foundation of Technology.

I thank Dr Cees Kranenburg for his suggestions, especially concerning the transformation of the consolidation equation from Eulerian to material coordinates.

Appendix A

Inflection point of the Reiner–Philippoff model

The mathematical formulation of the Reiner–Philippoff model reads

$$\boldsymbol{S}_d = -2\left[\eta_\infty + \frac{\eta_0 - \eta_\infty}{1 + \frac{\frac{1}{2}\mathrm{II}_{\boldsymbol{S}_d}}{\tau_0^2}}\right]\boldsymbol{D}_d, \tag{A.1}$$

which can be rewritten as

$$\mathrm{II}_{\boldsymbol{D}_d} = \left[\frac{-\frac{1}{2}}{\eta_\infty + \frac{\eta_0 - \eta_\infty}{1 + \frac{\frac{1}{2}\mathrm{II}_{\boldsymbol{S}_d}}{\tau_0^2}}}\right]^2 \mathrm{II}_{\boldsymbol{S}_d}. \tag{A.2}$$

Since (A.1) is symmetrical in the origin, it suffices to consider only the first quadrant. For this quadrant (A.2) can be written as

$$y = \left[\frac{-\frac{1}{2}}{\eta_\infty + \frac{\eta_0 - \eta_\infty}{1 + \frac{\frac{1}{2}x^2}{\tau_0^2}}}\right] x, \tag{A.3}$$

in which the substitutions $\mathrm{II}_{\boldsymbol{S}_d} = x^2$ and $\mathrm{II}_{\boldsymbol{D}_d} = y^2$ have been made. Differentiating (A.3) twice with respect to x and equating the result to zero, yields a condition for the inflection point. Solving for x and y gives

$$(x, y) = \left(\sqrt{6}\tau_0\sqrt{\frac{\eta_0}{\eta_\infty}}, \frac{\sqrt{6}}{8}\frac{(\eta_\infty + 3\eta_0)\tau_0}{\sqrt{\eta_\infty\eta_0}}\right) \tag{A.4}$$

or

$$(\mathrm{II}_{\boldsymbol{D}_d}, \mathrm{II}_{\boldsymbol{S}_d}) = \left(\frac{3}{32}\frac{(\eta_\infty + 3\eta_0)^2\tau_0^2}{\eta_\infty^3\eta_0}, \tau_0^2\frac{\eta_0}{\eta_\infty}\right). \tag{A.5}$$

Appendix B

The invariants of a second order tensor

In the present report, second order tensors are used to describe stress, deformation and deformation rate of materials in three dimensions. For simplicity these tensors are represented by one second order tensor $\boldsymbol{T}$:

$$\boldsymbol{T} = \begin{bmatrix} \tau_{11} & \tau_{12} & \tau_{13} \\ \tau_{21} & \tau_{22} & \tau_{23} \\ \tau_{31} & \tau_{32} & \tau_{33} \end{bmatrix}. \tag{B.1}$$

For reasons of spin momentum equilibrium the stress tensor must be symmetrical and with that the deformation (rate) tensor is symmetrical as well. This implies that $\tau_{ij} = \tau_{ji}$.

The the value of the elements of the tensor depend on the orientation of the carthesian coordinate system. However, for certain combinations of elements the value of these elements does not depend on the orientation of the coordinate system. These combinations are called the tensor's invariants. For the second order tensor $\boldsymbol{T}$ three invariants can be discerned. The three invariants are given by

$$\mathrm{I}_{\boldsymbol{T}} = \mathrm{Trace}(\boldsymbol{T}) = \tau_{11} + \tau_{22} + \tau_{33} = C_1, \tag{B.2}$$

$$\mathrm{II}_{\boldsymbol{T}} = \boldsymbol{T} : \boldsymbol{T} = \sum_i \sum_j \tau_{ij}\tau_{ji} = \tau_{11}^2 + \tau_{22}^2 + \tau_{33}^2 + 2\tau_{12}^2 + 2\tau_{13}^2 + 2\tau_{23}^2 = C_2, \tag{B.3}$$

$$\mathrm{III}_{\boldsymbol{T}} = \mathrm{Det}(\boldsymbol{T}) = \tau_{11}\tau_{22}\tau_{33} - \tau_{11}\tau_{23}^2 - \tau_{22}\tau_{13}^2 - \tau_{33}\tau_{12}^2 + 2\tau_{12}\tau_{23}\tau_{13} = C_3, \tag{B.4}$$

where C_i are constants.

For the stress tensor the constants C_i can be expressed in terms of principal stresses[1]. The values of the invariants become then

$$\mathrm{I}_{\boldsymbol{S}} = \sigma_1 + \sigma_2 + \sigma_3, \tag{B.5}$$

[1] In an arbitrary stress situation, a elementary cube of material can positioned in such a way that on none of its faces shear stresses are acting, but only normal stresses. In this situation the normal stresses are called principal stresses. The relative magnitude is expressed by the adjectives major, intermediate and minor.

$$\mathrm{II}_{\boldsymbol{S}} = \sigma_1^2 + \sigma_2^2 + \sigma_3^2, \tag{B.6}$$

$$\mathrm{III}_{\boldsymbol{S}} = \sigma_1 \sigma_2 \sigma_3, \tag{B.7}$$

where σ_1 represents the major principal stress, σ_2 represents the intermediate principal stress and σ_3 represents the minor principal stress. Similar expressions can be written for principal strain (rates).

It is noticed that if only the deviatoric tensors are considered, as is the case when incompressibility is assumed, then the first invariant is equal to zero by definition.

Yield stress condition

An arbitrary stress situation is considered. The orientation of the coordinate system is chosen such, that all normal stress components equal zero and all shear stress components are zero, but one. Then the shear stress is equal to the maximum shear stress τ_{max}. From (B.3) it follows that

$$2\tau_{\mathrm{max}}^2 = \mathrm{II}_{\boldsymbol{S}_d} \tag{B.8}$$

All models that incorporate yield stress, have the condition that $\boldsymbol{D} = 0\boldsymbol{I}$ when

$$\tau_{\mathrm{max}} < \tau_{\mathrm{y}}, \tag{B.9}$$

or, in terms of the second invariant

$$\tfrac{1}{2}\mathrm{II}_{\boldsymbol{S}_d} < \tau_{\mathrm{y}}^2. \tag{B.10}$$

List of Figures

List of Tables

List of Symbols

a	constant in Moore model	s^{-1}
a_v	coefficient of compressibility	Pa^{-1}
A_k	coefficient in (2.46)	–
A_p	coefficient in (2.45)	–
b	constant in Moore model	$Pa^{-1}\ s^{-1}$
B_k	coefficient in (2.46)	–
B_p	coefficient in (2.45)	–
c	constant in Moore model	Pa s
c	concentration	$kg\ m^{-3}$
c_u	maximum possible concentration	$kg\ m^{-3}$
c_m	concentration at which the function $F(c)$ has a minimum	$kg\ m^{-3}$
$\boldsymbol{D}$	strain rate tensor	–
$\boldsymbol{D}_d$	deviatoric strain rate tensor	–
e	void ratio	–
e_0	void ratio at zero effective stress	–
e_∞	void ratio at the end of consolidation	–
$\boldsymbol{E}$	strain tensor	–
$\boldsymbol{E}_d$	deviatoric strain tensor	–
g	acceleration due to gravity	$m\ s^{-2}$
G	coefficient in (2.43)	$m^2 s^{-1}$
$\boldsymbol{I}$	unity tensor	–
k	hydraulic conductivity (permeability)	$m\ s^{-1}$
K	total compression modulus	$kg\ m^{-1}\ s^{-2}$
K_s	compression modulus of particles	$kg\ m^{-1}\ s^{-2}$
m_a	amount of mass that is available to pass the control level	kg
m_p	amount of mass passed the control level	kg
p	pore water pressure	Pa
p_e	excess pore water pressure	Pa
p_{ss}	steady-state pore water pressure	Pa
$\boldsymbol{s}$	displacement	–
S	sediment flux	$kg\ m^{-2}\ s^{-1}$
$\boldsymbol{S}$	stress tensor	–
$\boldsymbol{S}_d$	deviatoric stress tensor	–

t	time	s
$\boldsymbol{T}$	arbitrary second order tensor	–
$\boldsymbol{u}$	velocity	m s^{-1}
U	interface velocity	m s^{-1}
v_f	velocity of fluid	m $^{-1}$
v_s	velocity of solids (settling velocity)	m s^{-1}
v_p	velocity of a single solid particle	m $^{-1}$
V	control volume	–
W	$= \frac{dS}{dc}$	m s^{-1}
x	(vertical) Eulerian coordinate	m
x_0	initial height	m
x'	integration variable for x	m
z	(vertical) material coordinate	m

β	coefficient in hindered settling function	–
β	interaction coefficient	–
δ_x	slice height	m
ε_{ij}	element (i,j) in the strain tensor	–
ε^*	compression	–
η_0	initial (constant) viscosity	Pa s
η_∞	viscosity at very high shear rates	Pa s
κ	dynamic bulk viscosity	Pa s
λ	coefficient in (2.48)	$kg^{-1}m\ s^2$
λ	structural parameter	–
λ_0	initial structural parameter	–
λ_e	equilibrium structural parameter	–
λ_s	super–structural parameter	–
ρ_f	density of fluid	kg m^{-3}
ρ_s	density of solids	kg m^{-3}
σ	total stress	Pa
σ_0	isotropic stress	Pa
σ_1	major principal stress	Pa
σ_2	intermediate principal stress	Pa
σ_3	minor principal stress	Pa
σ'	effective stress	Pa
τ	time	s
τ_d	dynamic yield stress	Pa
τ_s	static yield stress	Pa
τ_y	yield stress	Pa
τ_0	Bingham yield stress	Pa
τ_∞	yield stress at very high shear rates	Pa
ϕ_f	fluid fraction	–
ϕ_s	solid fraction	–

References

BEEN, K. 1980. *Stress-strain behaviour of a cohesive soil deposited under water.* Ph.D. thesis, Oxford University.

BILLINGTON, E. W. 1960. Some measurements of the time dependence of the viscosity of thixotropic fluids. *Proc. Phys. Soc.*, **75**, 40–50.

BIOT, M.A., & WILLIS, D.G. 1957. The elastic coefficients of the theory of consolidation. *J. Appl. Mech.*, **24**, 594–601.

BIRD, R.B., STEWART, W.E., & LIGHTFOOT, E.N. 1960. *Transport Phenomena.* Wiley, New York.

BOWDEN, R.K. 1988. *Compression behaviour and shear strength characteristics of a natural silty clay sedimented in the laboratory.* Ph.D. thesis, Oxford University.

CHENG, D.C-H. 1986. Yield stress: A time dependent property and how to measure it. *Rheologica Acta,*, **25**, 542–554.

CORNELISSE, J.M., KUIJPER, C., & WINTERWERP, J.C. 1993. *Analyse konsolidatieproeven en toepassing konsolidatiemodel met Ketelmeerslib.* Tech. rept. Rapport van Rijkswaterstaat en Waterloopkundig laboratorium.

COUSSOT, P., LEONOV, A.I., & PIAU, J.M. 1993. Rheology of concentrated dispersed systems in a low molecular weight matrix. *J. Non-Newtonian Fluid Mechanics*, **46**, 179–217.

GIBSON, R.E., ENGLAND, G.L., & HUSSEY, M.J.L. 1967. The theory of one-dimensional consolidation of saturated clays. *Géotechnique*, **17**, 261–273.

GIBSON, R.E., SCHIFFMAN, R.L., & CARGILL, K.W. 1981. The theory of one-dimensional consolidation of saturated clays. II Finite nonlinear consolidation of thick homogeneous layers. *Can. Geotech. J.*, **18**, 280–293.

HU, S. 1990. *Self-weight consolidation on impervious bases.* M.Phil. thesis, IHE, The Netherlands.

KYNCH, G.J. 1952. A theory of sedimentation. *Trans. Faraday Soc.*, **48**, 166–176.

MOORE, F. 1959. The rheology of ceramic slips and bodies. *Trans. Brit. Ceram. Soc.*, **58**, 470–494.

OLPHEN, H. VAN, & FRIPIAT, J.J. 1979. *Data handbook for clay materials and other non-metallic minerals.* Pergamon Press.

PANE, V., & SCHIFFMAN, R.L. 1985. A note on sedimentation and consolidation. *Géotechnique*, **35**(1), 69–72.

SKEMPTON, A.W. 1960. terzaghi's concept of effective stress. *Pages 42–53 of:* BJERRUM, L., CASAGRANDE, A., BECK, R.B., & SKEMPTON, A.W. (eds), *From theory to practice in soil mechanics.* John Wiley, New york.

TERZAGHI, K. 1943. *Theoretical Soil Mechanics.* John Wiley and Sons, New York.

TOORMAN, E.A. 1994. Towards a new consitutive equation for effective stress in self-weight consolidation. *In: Intercoh.*

TOORMAN, E.A. 1995. *The thixotropic behavior of dense cohesive sediment suspensions.* Tech. rept. Report HYD149, Hydraulics Laboratory, Katholieke Universiteit Leuven, Belgium.

TUNCAY, K., & CORAPCIOGLU, M.Y. 1995. Effective stress principle for saturated fractured porous media. *Water resources research*, **31**(12), 3103–3106.

VAN KESSEL, T. 1996. *Small-scale sounding tests on soft saturated cohesive soils.* Tech. rept. 7-96. Delft University of Technology.

VAN RIJN, L.C. 1990. *Priciples of fluid flow and surface waves in rivers, estuaties, seas and oceans.* Aqua publications, Amsterdam.

VERRUIJT, A. 1984. The theory of consolidation. *Pages 349–368 of:* J.BEAR, & CORAPCIOGLU, M.Y. (eds), *Fundamentals of transport phenomena in porous media.* Martinus Nijhoff, Norwell, Mass.

WORRALL, W.E., & TULIANI, S. 1964. Viscosity changes during the aging of clay-water suspensions. *Trans. Brit. Ceram. Soc.*, **63**, 167–185.